Equatorial wave intra-seasonal variability in the Indian and Pacific Oceans in the Mercator-Ocean POG05B simulation

By Serena Illig[1], Boris Dewitte[2], Claire Périgaud[1] and Corinne Derval[3]

[1] Jet Propulsion Laboratory (JPL/CALTECH), Pasadena, CA, USA
[2] LEGOS/IRD/IMARPE, Esquina de Gamarra y General Valle S/N Chucuito, Callao, Peru
[3] Cerfacs in Mercator Ocean - 8-10 rue Hermes. 31520 Ramonville St-Agne

Introduction

The tropical oceans have long been recognized as the most important region for large scale ocean-atmosphere interactions that give rise to coupled climate variations on several time scales. Whereas the tropical Atlantic and Pacific variability is the siege of air-sea interactions which characteristics are controlled to a large extend by equatorial wave dynamics (see *Latif et al.*, 1998) for the Pacific and *Xie and Carton* (2004) for a recent review for the tropical Atlantic), the tropical Indian ocean is rather subject to the strong forcing by the Indian Ocean monsoon that has a strong meridional component. This makes the equatorial wave response to the zonal wind stress more difficult to identify than in the other oceans. In the three oceans, equatorial waves were detected from observations (***Périgaud and Dewitte***, 1996; *Boulanger and Fu*, 1996; *Handoh and Bigg*, 2000; *LeBlanc and Boulanger*, 2001) and model simulations (*Dewitte et al.*, 2003; *Illig et al.*, 2004; ***Yuan and Han***, 2006) at seasonal to inter-annual timescales. To estimate the Kelvin and Rossby wave amplitude from altimetric data, the '*one-mode*' approximation which assumes that the surface data are representative of a single baroclinic mode, is required because the subsurface is insufficiently sampled to derive the vertical mode variability. Although there are limitations linked to the use of non-biases-free model and assimilation scheme, *Dewitte et al*. (2003) showed for the tropical Pacific that products with data assimilation can bring further insight for the interpretation of the altimetric data and surface variability associated to the equatorial waves. For the Indian and Atlantic Ocean, the '*one-mode*' approximation is anyway not valid due to the shallower thermocline and the peculiarities of the wind forcing. For instance, *Illig et al.* (2004) showed that 6 baroclinic modes are required at least to account for ~80% of the sea level variability.

In this study, we take advantage of the Mercator-Ocean effort to design a global system with data assimilation using the ORCA model (*Madec et al.*, 1998) to document the equatorial Indian Ocean vertical structure variability. Our study is based on the 'free' run (*i.e.* without data assimilation), which serves as a benchmark in order to assess the impact of data assimilation in future works. The paper identifies clear equatorial waves in the Indian Ocean and compares their characteristics to the ones in the Pacific Ocean focusing on the intra-seasonal variability.

Model simulation'description and validation

In this study, we used a free simulation for the period 1992-2001 (*Derval et al., 2005*) of the Mercator-Ocean global model (see *Dewitte et al.*, this issue, for a complete description of the simulation used). The simulation is referred to as POG05B hereafter.

Because equatorial wave depends on the mean stratification, the mean temperature and salinity field are first compared to observations from the World Ocean Atlas 2001 (*Conkright et al.*, 2002) (Figure 1). Figure 1 reveals known biases of many OGCMs, namely a too diffuse thermocline and a too salty warm pool. Overall, the simulated mean structure is rather realistic.

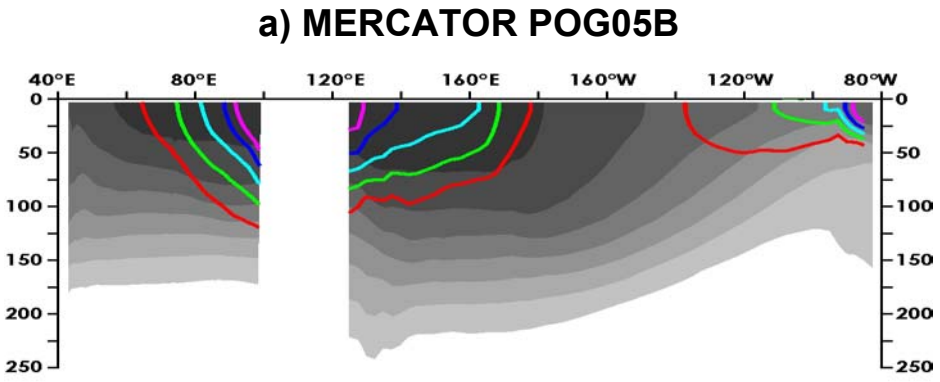

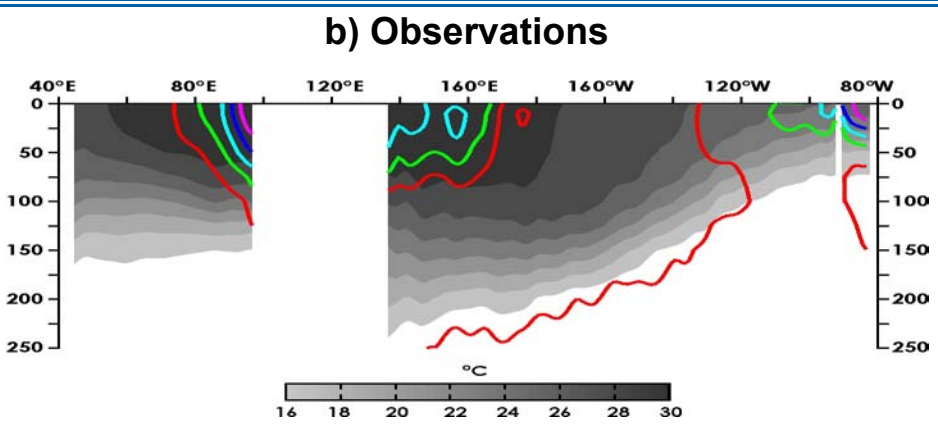

Figure 1

Equatorial mean structure within the first 250 meters over the tropical Indian-Pacific sector (1993-2001) for a) MERCATOR POG05B simulation and for b) the observations (World Ocean Atlas 2001). Grey shading represents the mean temperature section between 16°C and 30°C. 34, 34.25, 34.5, 34.75, 35 iso-salinity are represented with red, green, light blue, blue and purple solid lines respectively.

The model surface variability is then compared to satellite-derived observations, the TOPEX/Poseidon and ERS-1/2 combined data sets from October 1992 to January 2002 (*Ducet et al.*, 2000) and the OSCAR current anomaly. OSCAR provides near-surface currents derived from satellite altimeter, scatterometer and SST (*Bonjean and Lagerloef*, 2002). The surface layer current is the sum of geostrophic and Ekman currents and of a buoyancy term. The comparison indicates that the model simulate fairly well the surface variability in the equatorial band, with on average more skill in the Pacific than in the Indian oceans (Figure 2a) due to the energetic inter-annual variability in the Pacific (representative of ENSO) which is more easily grasped by the model than in the Indian ocean. Similar analysis on the high-pass filtered outputs (figure 2b) reveals however that the model simulate fairly well the intra-seasonal variability in the Indian ocean with correlation level as large as in the Pacific ocean for sea level and larger by ~0.1 on average than in the Pacific ocean for the surface currents.

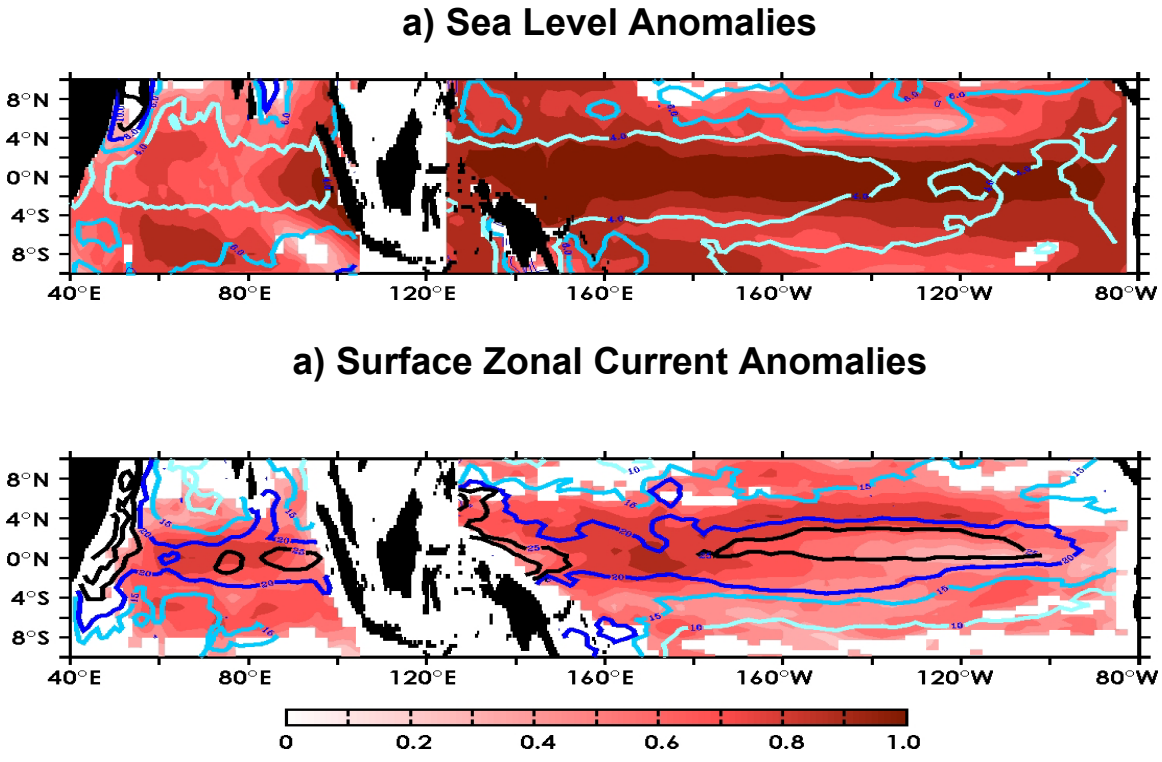

Figure 2a

Comparison between POG05B and independent satellite observations over the tropical Indian-Pacific sector over the 1993-2001 period. Sea Level (top panel) and Surface zonal current (bottom panel) inter-annual anomalies 99% significant correlations (red-shaded) as well as RMS differences between model and AVISO merged sea level (OSCAR surface currents) (color contours) are shown. Contour intervals are 2 *cm* for Sea Level RMS and 5 *cm/s*.for zonal current RMS.

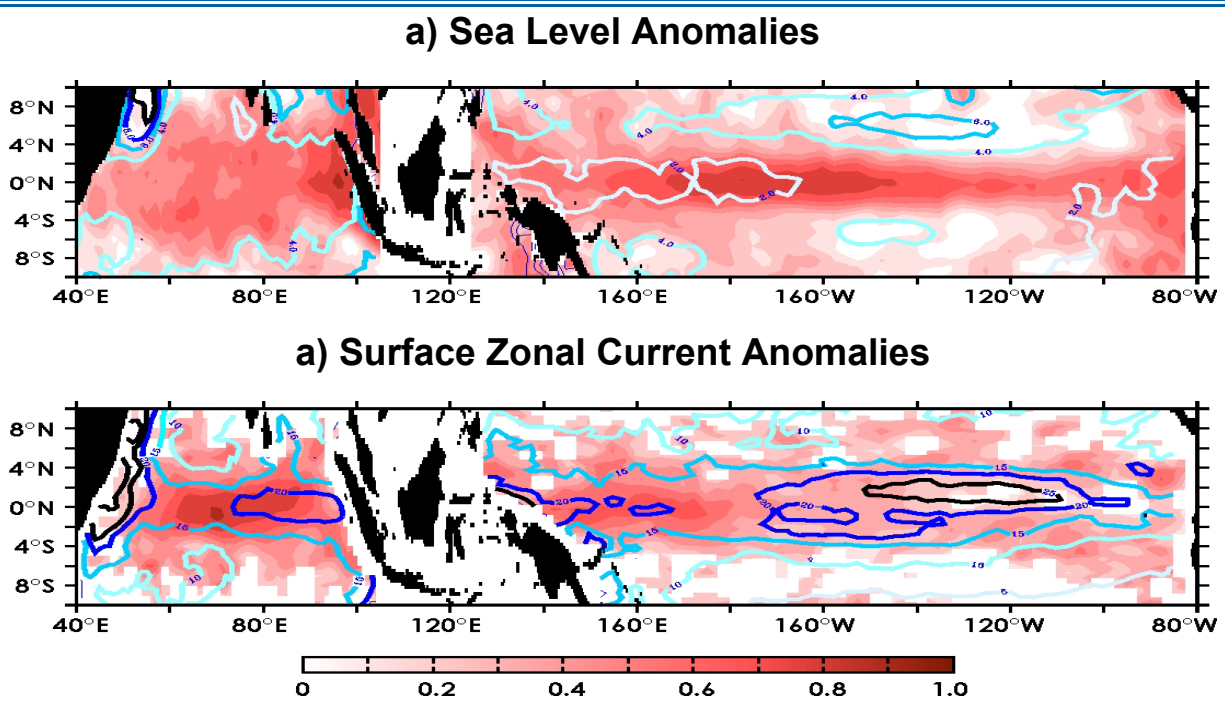

Figure 2b

Same as Figure 2a, but for the high-pass filtered data (*fc*= (150) *days*$^{-1}$).

Vertical structure variability and wave sequences

A vertical mode decomposition of the model mean stratification is sought following *Dewitte et al.* (1999) and baroclinic mode contribution to pressure and current anomalies are derived, which then allows inferring the Kelvin and Rossby wave amplitudes. Such method was used in previous studies for the equatorial Pacific (*Dewitte el al.*, 1999; 2003) and Atlantic (*Illig et al.* 2004). It is extended here for the case of the Indian Ocean.

Baroclinic mode contributions

We first analyze the characteristics of the baroclinic modes variability in terms of surface zonal current. The total Zonal Current Anomalies (ZCA) are estimated by averaging the currents over the 4 uppermost levels of the model (5–30 m depth), in order to remove the shear within the weakly stratified surface layer associated with incomplete mixing which cannot be represented in the vertical mode decomposition. The RMS variability of the surface ZCA is presented in Figure 3a.

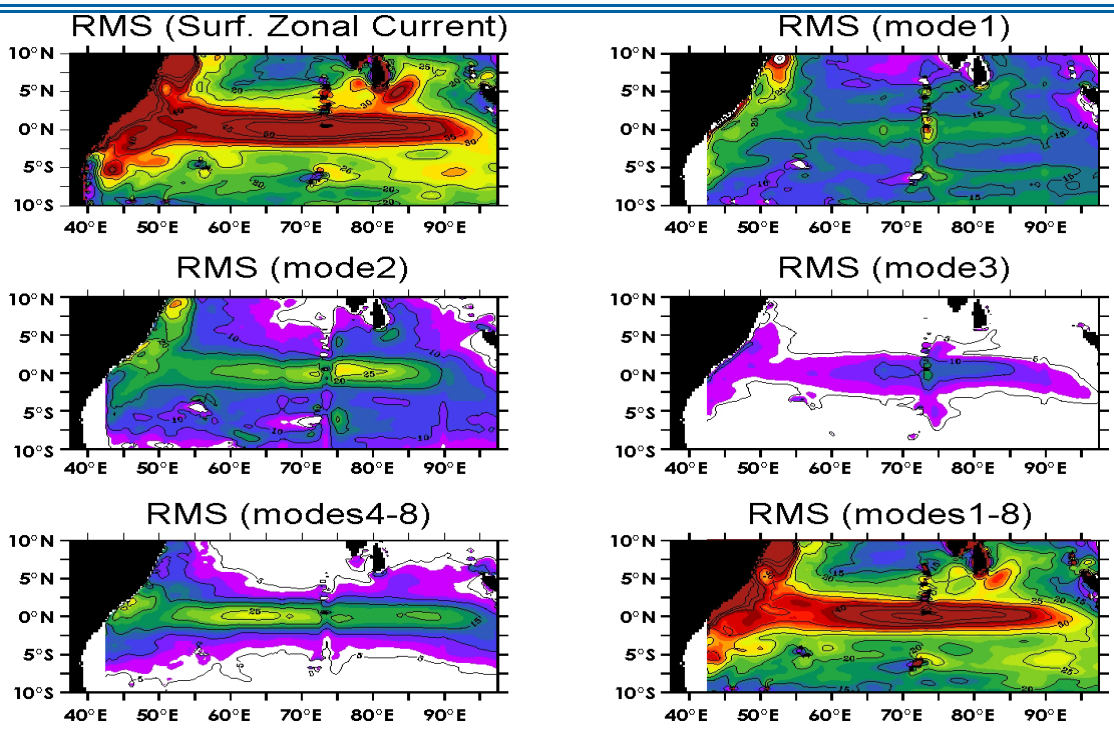

Figure 3

Maps of variability (RMS) over 1993-2001 of (a) MERCATOR POG05B total surface zonal currents, (b-d) the contribution of the three first baroclinic modes, (e) the summed-up contribution of the high order baroclinic modes (4-8), and (f) the sum of the 8 gravest baroclinic modes. Contour interval is 5 *cm/s*. Values smaller than 6 *cm/s* appear in white;

Large values (>50 $cm.s^{-1}$) are confined within 2°S–2°N, with maximum variability centered around 75°W and in the western boundary current system. The results of the vertical mode decomposition of the zonal current variability (Figures 3b-f) indicate that the current variability project over a large number of modes, with the second baroclinic mode being the most energetic in the central basin. Interestingly, the wind projection coefficient along the equator is 0.73, 0.56, 0.18 and 0.32 for the first, second, third and fourth baroclinic mode on average in the western basin indicating that the mean stratification should favour the first baroclinic mode. This suggests a specific pattern of the wind forcing which amplify the second baroclinic mode contribution or the presence of resonant modes. The second baroclinic mode is indeed expected to resonate at the 60, 90 and 180 $days^{-1}$ frequencies, timescales that are present in the wind forcing over the Indian Ocean (Shinoda et al., 1998).

The explained variances of the mode contribution to sea level anomalies are on average along the equator 30%, 15%, 5% and 60% for respectively the first, second, third and the summed-up contributions of modes 1 to 8 for both the total and high-passed filtered (fc=150 $days^{-1}$) variability.

Wave sequences

Projecting the baroclinic mode contributions to zonal current and sea level anomalies onto the theoretical Kelvin and Rossby wave structures provide an estimation of the equatorial wave amplitude (*Illig et al.*, 2004). The figures 4 and 5 display the result of the decomposition (second baroclinic mode) for both the total and high-pass filtered outputs. Clear propagations of the sea level anomaly can be observed.

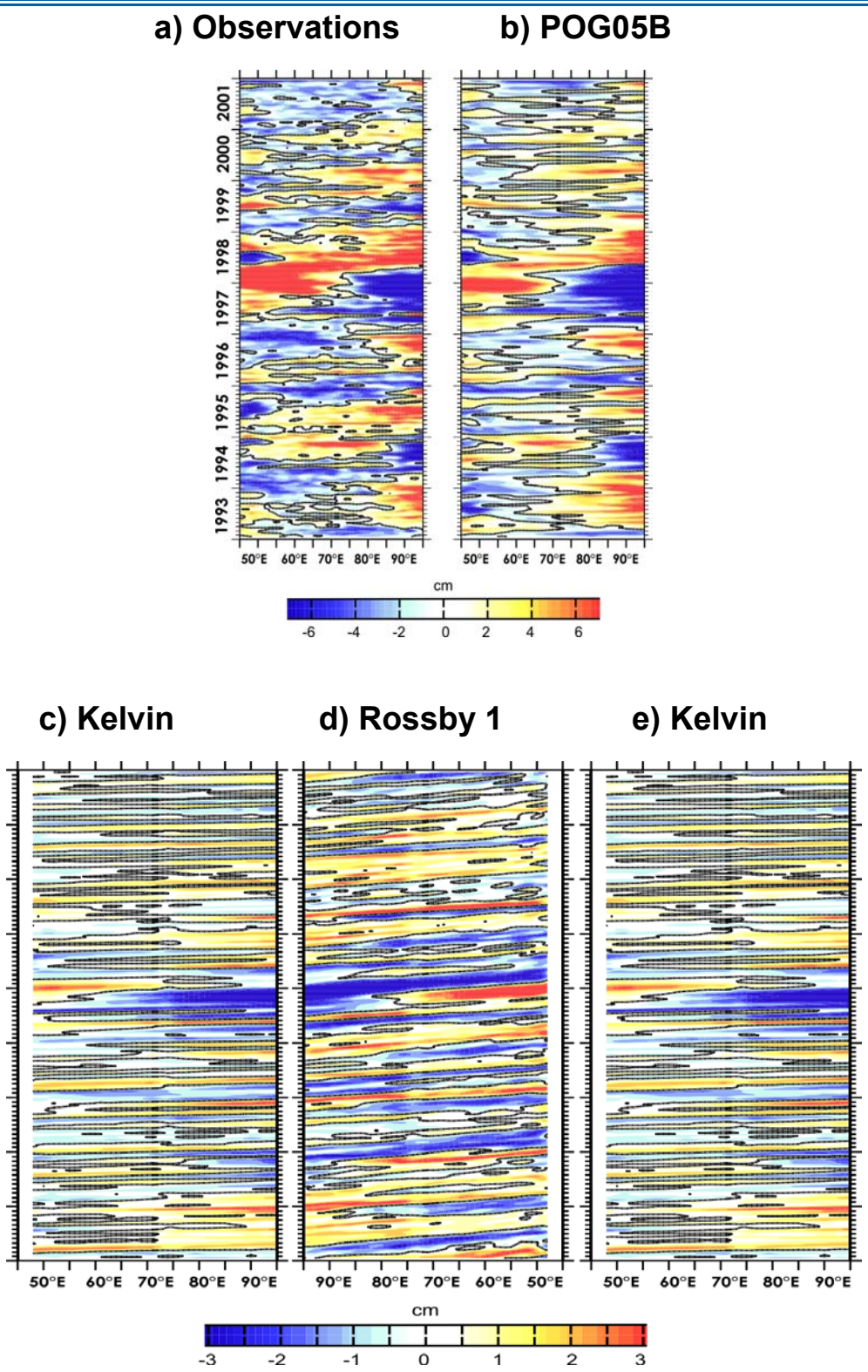

Figure 4:

Longitude-time plot of the seal level anomalies for a) the altimetric data (at 0°N), for b) the POG05B simulation (at 0°N), for c/e) the Kelvin wave contribution (K at 0°N) and the first meridional Rossby component (R1 at 3°S) for the second baroclinic mode. R1 is displayed reverse from 99°E to 43°E and K is repeated in order to visualize the reflection at the eastern and western basin boundaries. Positive (negative) values are red (blue) shaded respectively.

They are associated to the main sea level anomalies during this period, in particular during the 1997/98 El Niño event (figure 4). Whereas the 1997/98 El Niño in the Pacific is associated to the forcing of energetic downwelling Kelvin waves (*Dewitte et al.*, 2003), in the Indian equatorial Ocean, upwelling Kelvin are forced in 1997 (figure 4c) which reflects at the eastern boundary as Rossby waves (figure 4d).

POG05B also simulate propagations of equatorial waves at intra-seasonal frequencies (figures 5cde).

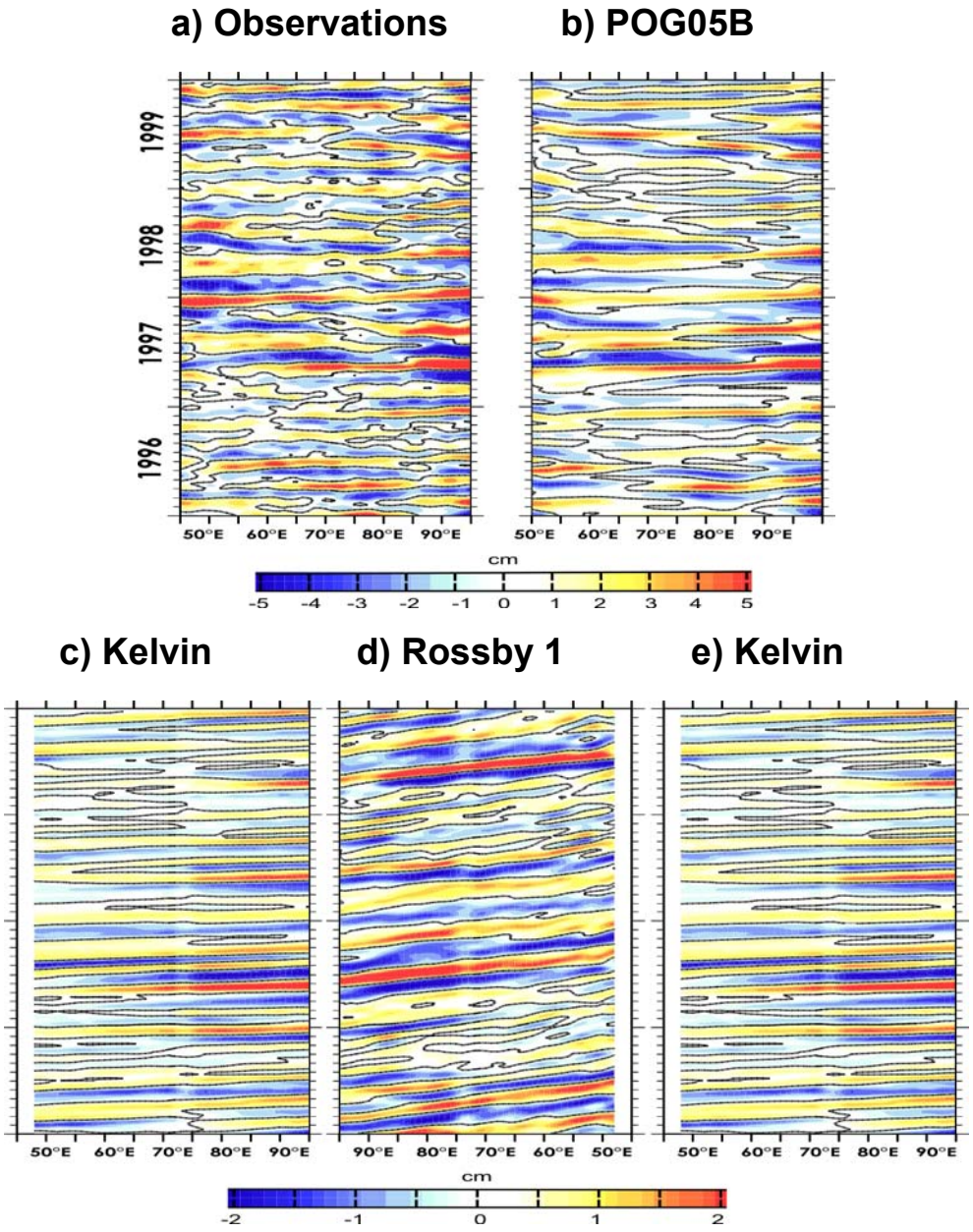

Figure 5

Same as figure 4 but for the high-pass filtered anomalies (fc= (150) days^{-1}).

Intra-seasonal variability and role of boundary reflections

Wavenumber-frequency diagrams

In order to analyze the propagating nature of the estimated Kelvin and Rossby components, a bivariate space-time spectral analysis (*Hayashi*, 1977) is applied on the high-pass filtered POG05B outputs along the equator (for the Kelvin wave) and along 3°S (for the 1st meridional Rossby wave component R1 wave) for the first two energetic baroclinic modes. Results are displayed in figures 6 and 7 for the Indian and Pacific Oceans respectively. The diagrams reveal the presence of long-wave length (k<2)

Kelvin at ~150, ~100 and ~60 (*days*)$^{-1}$ in the Indian Ocean. Counterparts can be found in the 1st-meridional Rossby component for both baroclinic modes suggesting resonance of the waves at these frequencies. On the other hand, the analysis for the Pacific ocean only exhibit energetic peaks for the Kelvin wave and to a lesser extent for the first baroclinic mode Rossby wave at ~150 *days*$^{-1}$ (which is believed to be a residual of the semi-annual cycle) indicating that the Kelvin wave is mostly forced at these frequencies.

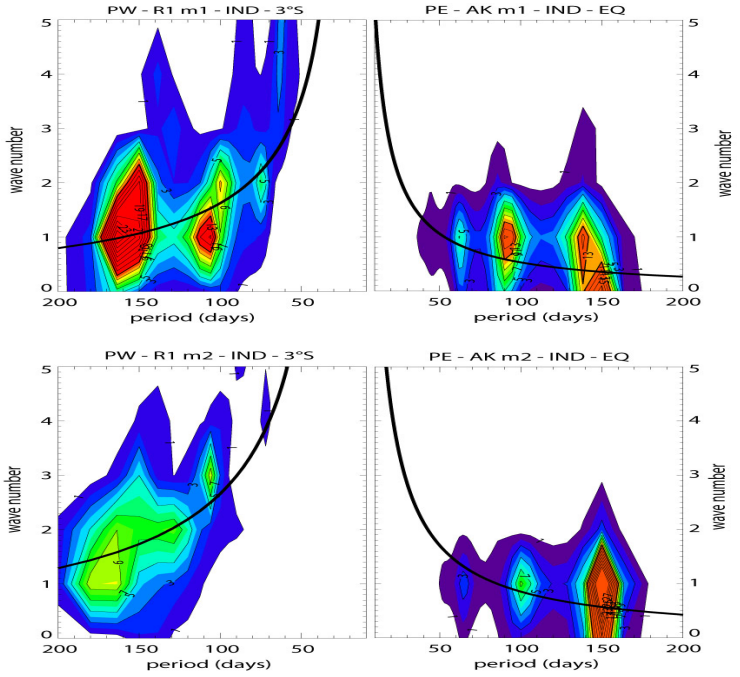

Figure 6

The space-time power spectral density of the 6-month high-pass filtered Kelvin waves (at the equator) and first-meridional Rossby (R1) waves (along 3°S) in the Indian Ocean for the (top panels) first and (bottom panels) second baroclinic modes. Theoretical dispersion curves for Kelvin and R1 waves using the zonally averaged phase velocity as derived from the vertical mode decomposition are plotted in thick black lines.

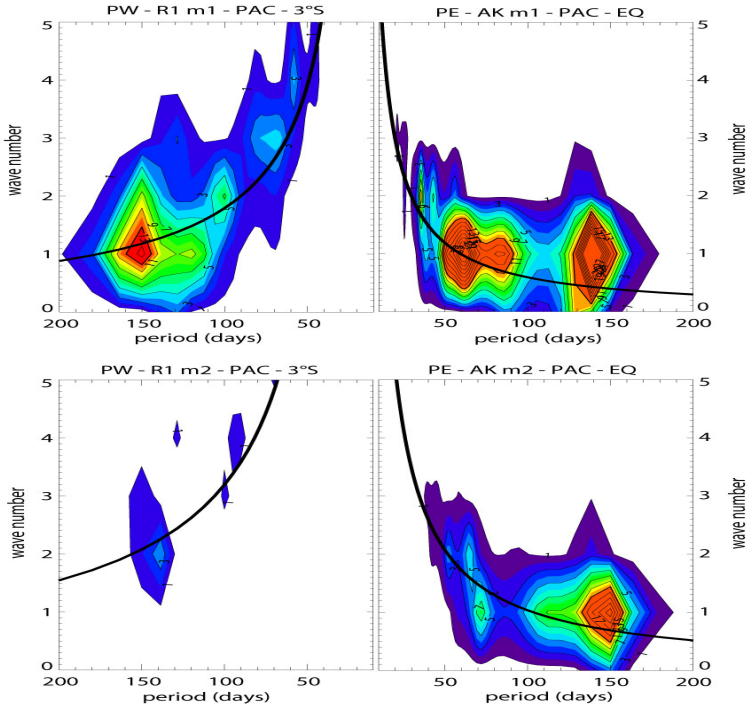

Figure 7

Same as Figure 6 but for the Pacific Ocean.

Role of boundary reflections

	Phase speed (c_n) in *m/s*	Wind projection coefficients
Mode 1	2.72	0.73
Mode 2	1.71	0.56
Mode 3	0.95	0.18
Mode 4	0.74	0.32
Mode 5	0.57	0.15
Mode 6	0.47	0.28
Mode 7	0.41	0.17
Mode 8	0.36	0.23

Table 1

Baroclinic mode characteristics of the linear model of the equatorial Indian ocean (ILIN). The values are estimated from the time averaged phase speed and wind projection coefficients at [80°E-85°E; 0°N] of the 8 gravest baroclinic modes as derived from the POG05B vertical decomposition. Wind projection coefficient is adimensionalized by 150m.

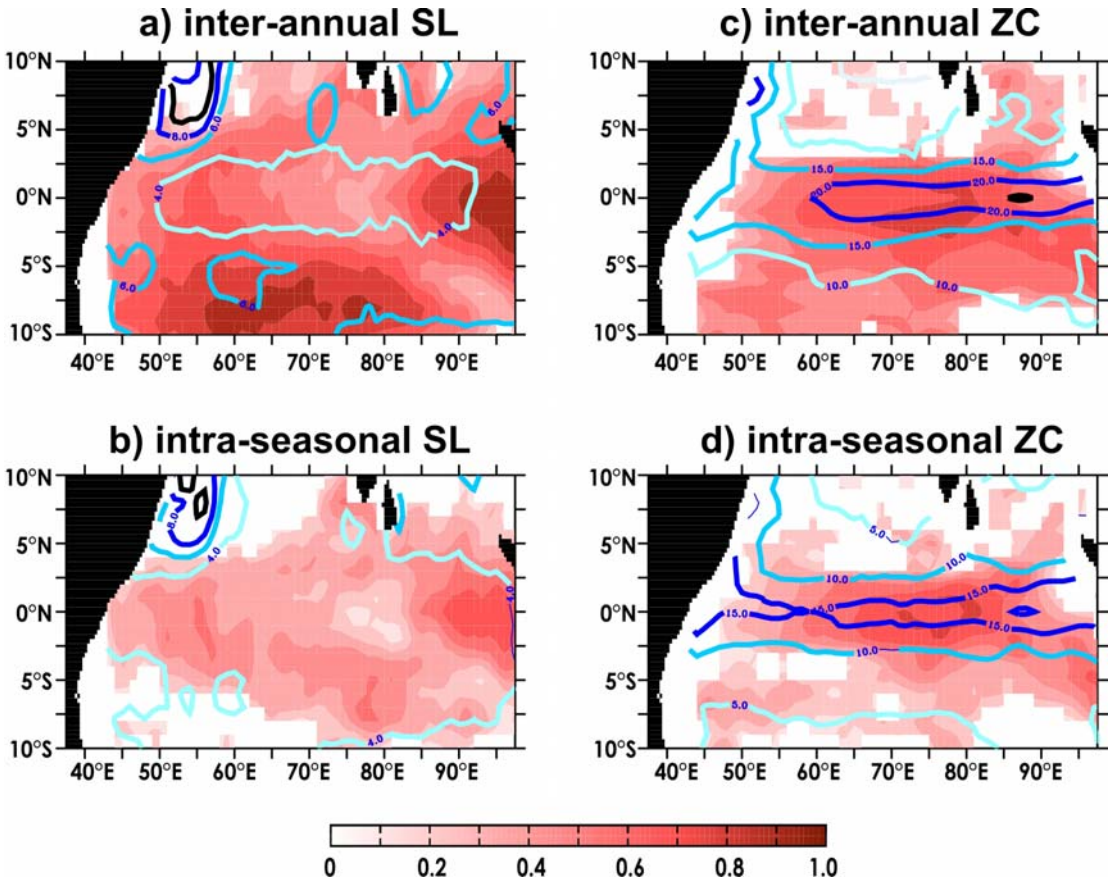

Figure 8

Comparison between the Indian Linear Model (ILIN) and independent satellite observations over the tropical Indian sector over the 1993-2001 period. Inter-annual (top panels) and intra-seasonal (bottom panels) Sea Level (left panels) and Surface Zonal Current (right panels) correlations (red-shaded) and RMS differences between model and AVISO merged sea level (OSCAR surface currents) (color contours) are shown. Contour interval is 2 *cm for Sea Level RMS and* 5 *cm/s* for Surface Zonal Current RMS. Only correlations significant at the 99% level are displayed

A linear model of the Indian equatorial Ocean (hereafter ILIN) is designed taking advantage of the information provided by the vertical mode decomposition of POG05B.

The model is composed of 8 baroclinic modes with characteristics similar to POG05B (see Table 1). The model is validated from satellite observations (Figure 8), which indicates that it is as skilful as POG05B for simulating the surface current and sea level variability in the equatorial band (compare Figure 8 with Figures 1 and 2). This validates the results of the vertical mode decomposition presented above and allows for sensitivity tests with the model to study the role of equatorial waves at the meridional boundaries on the surface variability. In particular ILIN offers the opportunity to test the resonant character of the baroclinic modes. In the Indian Ocean, because of its narrow span, there is the possibility that intra-seasonal equatorial waves are forced through a resonance effect caused by stationary or slowly propagating patches of wind (Kessler et al., 1995). Cancelling out the reflection efficiency at the meridional boundary in ILIN will provide insight on such process. Such an experiment is carried out. Results are compared to the control experiment (*i.e.* considering full efficiency at the meridional boundary).

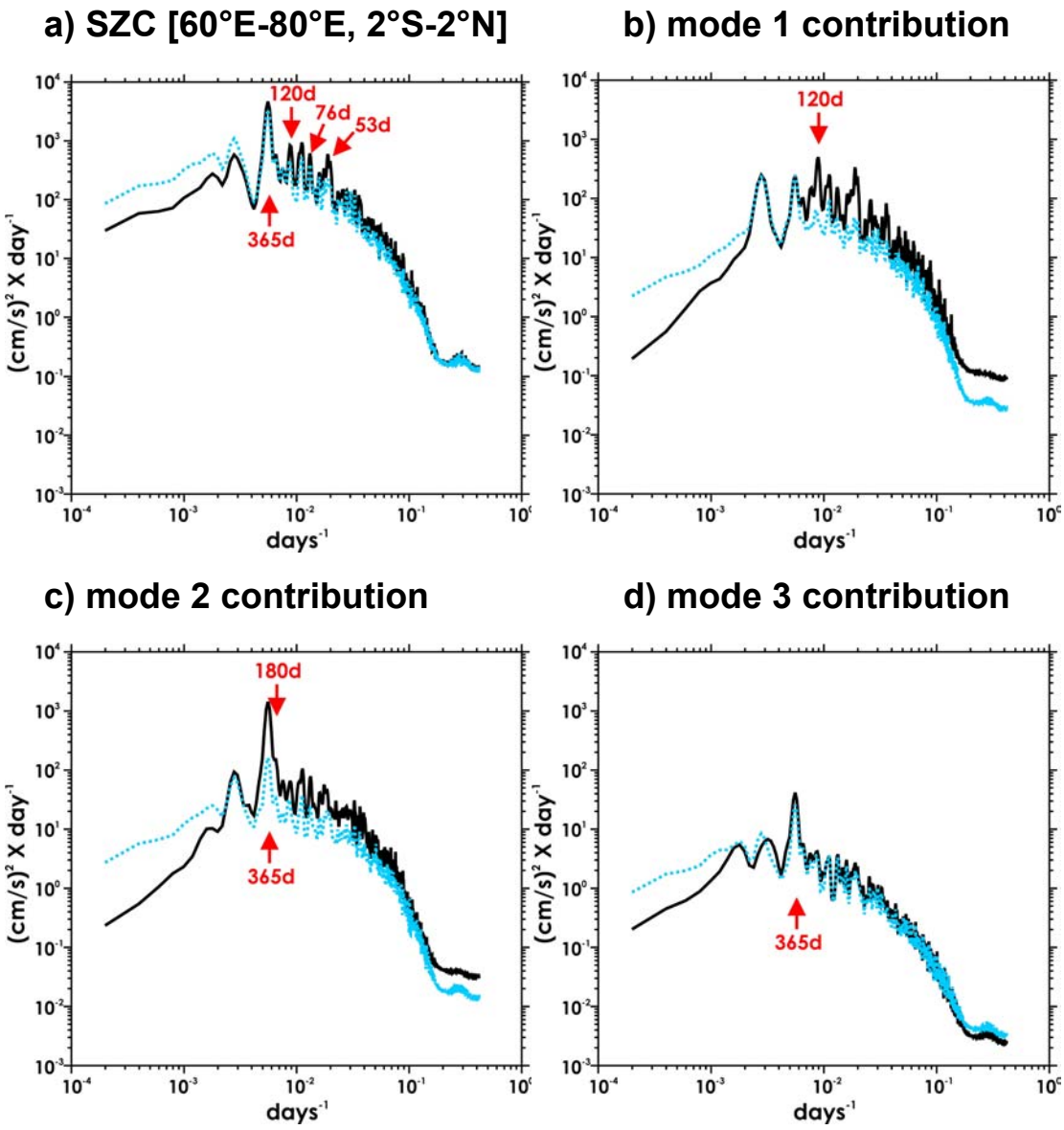

Figure 9

Mean conservative spectrum [60°E-80°E, 2°S-2°N] of the ILIN Surface Zonal Current (SZC) estimated by autocorrelation for a) the total ZSC, b-d) the contribution of the 3 gravest baroclinic modes respectively. The plain black (dashed blue) line respectively corresponds to the control experiment ('no reflection' experiment).

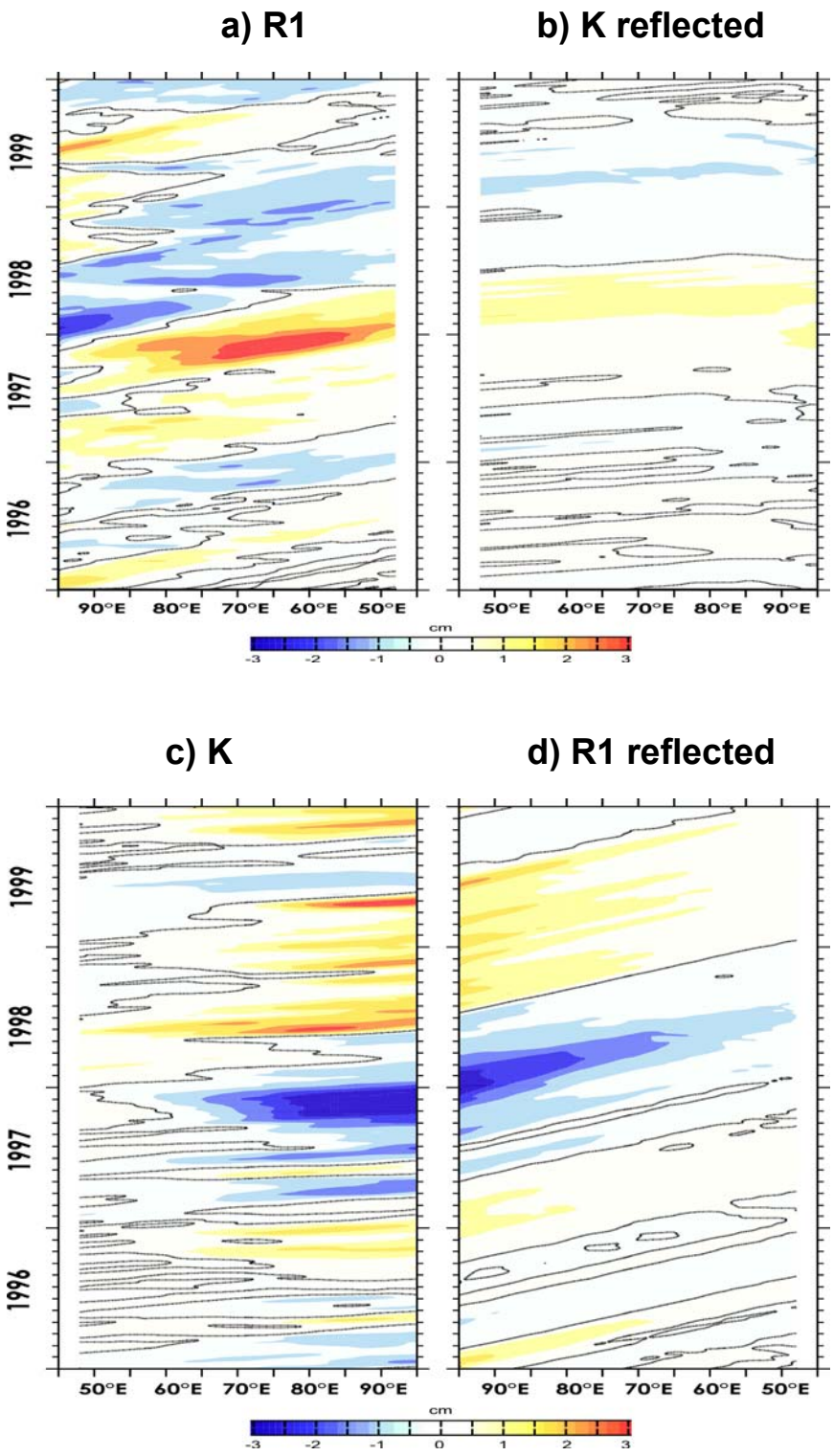

Figure 10

Longitude-time plot of the second baroclinic mode contributions to the sea level anomalies simulated by the Indian Linear Model (ILIN): a) first meridional Rossby component (R1) at 3°S, b) reflected Kelvin wave contribution at 0°N, c) Kelvin wave component (K) at 0°N and d) reflected R1 contribution at 3°S. R1 is displayed reverse from 99E to 43E in order to visualize the reflection at the western and eastern basin boundaries. Positive (negative) values are red (blue) shaded respectively.

Figure 9 displays the spectrum of the simulated surface current anomalies in the central equatorial Indian Ocean. Figure 9a exhibits significant differences between the control experiment and the simulation without reflection at the boundary in particular at the frequencies ~180 and ~120, at which resonance is expected. The spectra of the gravest baroclinic mode contributions (figure 9b-d) show that the faster and less dissipative the baroclinic mode is, the more important the impact of the reflection at the meridional boundaries is. For the first and the second baroclinic modes (the most energetic), the impact on the intra-seasonal frequencies is significant: along with the specific resonance (120 and 180 *days* respectively) of each mode the reflection intensifies the wind energy in the intra-seasonal frequency band. For the high order baroclinic modes the impact becomes less noticeable.

The difference between both experiments allows estimating the contribution of the reflected Kelvin and Rossby waves (Figure 10). Although such estimate is dependent of some arbitrary choice on the dissipation coefficient (see *Illig et al.* (2004) for details), figure 10 suggests that the contributions of the reflected waves can reach the central basin with significant amplitude. Organized intra-seasonal wind forcing may then amplify the Kelvin wave at the resonant frequencies.

Discussion and conclusions

Equatorial waves in the Indian Ocean were clearly identified thanks to a vertical mode decomposition of the POG05B simulation. The analysis focuses on the intra-seasonal variability which is the dominant component of the surface variability in the Indian equatorial ocean. The results indicate that equatorial waves in the Indian Ocean have a significant contribution to the surface variability in terms of sea level and currents. The second baroclinic mode waves are the most energetic although the mean equatorial stratification favour the forcing of first baroclinic mode. The comparison with similar analysis over the equatorial Pacific ocean allows documenting the peculiarities of the results with respect to the nature of the wave (resonant versus forced). It is found that, whereas the intra-seasonal Kelvin wave is mostly forced by the wind in the Pacific Ocean, in the Indian Ocean, resonance of the waves takes place leading to energetic variability of the Rossby waves and surface current variability. Sensitivity experiments using a linear ocean model of the equatorial Indian Ocean support the above interpretation. The linear model is in particular as skilful as the OGCM for simulating the surface variability in the equatorial band supporting the interpretation of the variability in terms of long wavelength waves and resonance modes.

The issue of the relationship between intra-seasonal wind forcing and the equatorial oceanic Kelvin waves has drawn a lot of interest in recent years mostly because intra-seasonal variability in the western Pacific and Indian oceans is tightly link to ENSO triggering and development (Kessler et al., 1995). It has been suggested that this relationship must be strongly nonlinear because of the differing frequencies (*Kutsuwada and McPhaden*, 2002) but the nonlinear processes that couple these modes are not fully understood. The results reported here suggest that in the Indian equatorial ocean, superposition of linear waves with a specific vertical structure and their reflections at the meridional boundaries may explain the enhancement of the surface current variability at the resonant frequencies.

Overall, we have proposed and validated a methodology for deriving equatorial waves in the Indian Ocean using the POG05B Mercator-Ocean global simulation. Similar diagnostics applied to products with data assimilation based on the POG05B model version should bring further insights on the pertinence of our approach along with providing metrics of the impact of the assimilation, which in turn will allow resolving the scientific issues rose in this study.

Acknowledgements

We thank Eric Greiner for his support and for fruitful discussions during the course of this study.

References

Bonjean, F. and G. S. E. Lagerloef, 2002: Diagnostic model and analysis of the surface currents in the tropical Pacific ocean. *J. Phys. Oceanogr.*, 32 (10), 2938–2954.

Boulanger J. P., and L.-L. Fu, 1996: Evidence of boundary reflection of Kelvin and first-mode Rossby waves from TOPEX/Poseidon sea level data. *J. Geophys. Res.,* **101,** 16 361–16 371.

Conkright, M. E., R. A. Locarnini, H. E. Garcia, T. D. O'Brien, T. P. Boyer, C. Stephens, and J. I. Antonov, 2002: World Ocean Atlas 2001: Objective Analyses, Data Statistics, and Figures [CD-ROM], NOAA, Silver Spring, Md.

Derval C, Durand E., Garric G. and E. Remy, 2005 : Dossier technique d'experimentation ORCA-R025 POG-05B , Mercator-Ocean internal report.

Dewitte B., G. Reverdin and C. Maes, 1999: Vertical structure of an OGCM simulation of the equatorial Pacific Ocean in 1985-1994.*J. Phys. Oceanogr.*, **29**, 1542-1570.

Dewitte B., S. Illig, L. Parent, Y. duPenhoat, L. Gourdeau and J. Verron, 2003: Tropical Pacific baroclinic mode contribution and associated long waves for the 1994-1999 period from an assimilation experiment with altimetric data. *J. Geophys. Research.,* 108 (C4), 3121-3138.

Ducet, N., P. Le Traon, and G. Reverdin, 2000: Global high resolution mapping of ocean circulation from Topex/Poseidon and ERS-1/2, *J. Geophys. Res*., 105, 19477-19498.

Handoh, I.C. and G.R. Bigg, 2000: A self-sustaining climate mode in the tropical Atlantic, 1995-1997: Observations and modelling, *Q. J. R. Met. Soc*., 126, 807–821.

Hayashi, Y., 1977: Space-time power spectral analysis using the maximum entropy method, *J. Meteorol. Soc. Japan*, **55**, 415-420.

Illig S., B. Dewitte, N. Ayoub, Y. du Penhoat, G. Reverdin, P. De Mey, F. Bonjean and G.S. E. Lagerloef, 2004: Inter-annual Long Equatorial Waves in the Tropical Atlantic from a High Resolution OGCM Experiment in 1981-2000. *J. Geophys. Research.,* **109**, No. C2, C02022, doi:10.1029/2003JC001771.

Jakobsson, M., N.Z. Cherkis, and J.W.R.M.B. Coakley, (2000), New grid of Arctic bathymetry aids scientists and mapmakers., *Eos, Transactions, American Geophysical Union*, *81(9)*, 89-93-96.

Jourdan, D., E. Balopoulos, M.J. Garcia-Fernandez, and C. Maillard, *Objective Analysis of Temperature and Salinity Historical Data Set over the Mediterranean Basin*, (1998), IEEE.

Kessler, W. S., M. J. MacPhaden, and K. M. Weickmann, 1995: Forcing of intraseasonal Kelvin waves in the equatorial Pacific. *J. Geophys. Res.*, 100, 10613-10631.

Kutsuwada, K., and M. McPhaden, 2002: Intraseasonal variations in the upper equatorial Pacific Ocean prior to and during the 1997-98 El Niño. *J. Phys. Oceanogr.*, **32**, 1133-1149.

Latif, M., D. Anderson, T. Barnett, M. Cane, R. Kleeman, A. Leetma, J. O'Brien, A. Rosati, and E. Schneider, 1998: A review of the predictability and prediction of ENSO. *J. Geophys. Res*., 103(C7), 14375-14393.

Le Blanc, J. L., and J. P. Boulanger, 2001: Propagation and reflection of long equatorial waves in the Indian Ocean from TOPEX/Poseidon data during the 1993–1998 period. *Climate Dyn.,* **17,** 547–557.

Levitus, S., T.P. Boyer, M.E. Conkright, T. OBrian, J.I. Antonov, C. Stephens, L. Stathopolos, D. Johnson, and R. Gelfeld, *World Ocean Database 1998 - NOAA Atlas NESDID18*, (1998), National Oceanographic Data Center, Silver Spring, MD.

Lythe, M., D.G. Vaughan, and B. Consortium, (2001), BEDMAP: a new ice thickness and subglacial topographic model of Antarctica., *J. Geophys. Res.*, *106*, 11335-11352.

Madec, G., P. Delecluse, M. Imbard, and C. Levy, *OPA 8.1 general circulation model reference manual*, (1998), Notes de l'Institut Pierre-Simon Laplace (IPSL) - Universite P. et M. Curie, B102 T15-E5, 4 place Jussieu, Paris cedex 5, 91p.

Madec, G., and M. Imbard, (1996), A global ocean mesh to overcome the North Pole singularity, *Clim. Dyn.*, *12*, 381-388.

Périgaud C. and B. Dewitte, 1996: El Niño-La Niña events simulated with the Cane and Zebiak's model and observed with satellite or in situ data. Part I: Model and data comparison. *J. Climate*, **9**, 66-84.

Shinoda, T., H. H. Hendon, and J. Glick, 1998: Intraseasonal variability of surface fluxes and sea surface temperature in the tropical western Pacific and Indian Oceans. *J. Climate*, **11**, 1685-1702.

Smith, W.H.F., and D.T. Sandwell, (1997), Global sea-floor topography from satellite altimetry and ship depth soundings., *Science*, *277*, 1956-1962.

Steele, M., R. Morley, and W. Ermold, (2001), PHC: A global ocean hydrography with a high quality Arctic Ocean., *Journal of Climate*, *14*, 2079-2087.

Uppala, S., (2001), ECMWF Reanalysis, 1957-2001, ERA-40 - Proceedings of workshop Re-analysis, 5-9 november, ECMWF, Reading.

Xie, S.-P., and J. A. Carton, 2004: Tropical Atlantic variability: Patterns, mechanisms, and impacts. *Earth Climate: The Ocean-Atmosphere Interaction, Geophys. Monogr.,* Vol. 147, *Amer. Geophys. Union*, 121–142.

Yuan D. and W. Han, 2006: Roles of Equatorial Waves and Western Boundary Reflection in the Seasonal Circulation of the Equatorial Indian Ocean, J. Phys. Oceanogr. 36, 930-944.

Notebook

Editorial Board :

Laurence Crosnier

Secretary :

Monique Gasc

Articles:

News1 : EGEE campaigns during the African monsoon multidisciplinary analysis program

By Bernard Bourlès

News2: Tropical arrays for observing ocean and atmosphere dynamics

By Fabrice Hernandez

The new 1/4° Mercator-Ocean global multivariate analysis and forecasting system: Tropical oceans outlook

By Marie Drévillon, Laurence Crosnier, Nicolas Ferry, Eric Greiner and the PSY3V2 Team

"Bulletin Climatique Global" of Météo-France; a contribution of Mercator-Ocean to the seasonal prediction of El Niño 2006-07

By Silvana Ramos Buarque , Christophe Cassou, Isabelle Charon and Jean-François Gueremy

Structure of intra-seasonal variability in the upper layers of the equatorial Atlantic Ocean from the Mercator-Ocean MERA-11 reanalysis

By Frédéric Marin, Gabriel Athié, Charly Régnier and Yves du Penhoat

Connexion between the equatorial Kelvin wave and the extra tropical Rossby wave in the South Eastern Pacific in the Mercator-Ocean POG05B simulation: a case study for the 1997/98 El Niño

By Boris Dewitte, Marcel Ramos, Oscar Pizarro and Gilles Garric

Equatorial wave intra-seasonal variability in the Indian and Pacific Oceans in the Mercator-Ocean POG05B simulation

By Serena Illig, Boris Dewitte, Claire Périgaud and Corinne Derval

Contact :

Please send us your comments to the following e-mail address: webmaster@mercator-ocean.fr

Next issue: October 2007